Available online at www.sciencedirect.com
ScienceDirect
Phytochemistry 68 (2007) 2341–2350
PHYTOCHEMISTRY
www.elsevier.com/locate/phytochem

In vivo ^{13}C NMR determines metabolic fluxes and steady state in linseed embryos

Stéphanie Troufflard [a,1], Albrecht Roscher [a,*], Brigitte Thomasset [b], Jean-Noël Barbotin [a], Stephen Rawsthorne [c], Jean-Charles Portais [d,e]

[a] *Génie Enzymatique et Cellulaire, UMR-CNRS 6022, Université de Picardie Jules Verne, 33 Rue St-Leu, 80039 Amiens, France*
[b] *Génie Enzymatique et Cellulaire, UMR-CNRS 6022, Université de Technologie de Compiègne, B.P. 20529, 60205 Compiègne, France*
[c] *Department of Metabolic Biology, John Innes Centre, Norwich Research Park, Colney, Norwich NR4 7UH, United Kingdom*
[d] *UMR5504, UMR792 Ingénierie des Systèmes Biologiques et des Procédés, CNRS, INRA, INSA, 31400 Toulouse, France*
[e] *Université Paul Sabatier, Toulouse, France*

Received 23 February 2007; received in revised form 15 April 2007
Available online 30 May 2007

Abstract

The dynamics of developing linseed embryo metabolism was investigated using ^{13}C-labelling experiments where the real-time kinetics of label incorporation into metabolites was monitored *in situ* using *in vivo* NMR. The approach took advantage of the occurrence in this plant tissue of large metabolite pools – such as sucrose or lipids – to provide direct and quantitative measurement of the evolution of the labelling state within central metabolism. As a pre-requisite for the use of steady state flux measurements it was shown that isotopic steady state was reached within 3 h at the level of central intermediates whereas it took a further 6 h for the sucrose pool. Complete isotopic and metabolic steady state took 18 h to be reached. The data collected during the transient state where label was equilibrated but the metabolic steady state was incomplete, enabled the rates of lipid and sucrose synthesis to be measured *in situ* on the same sample. This approach is suitable to get a direct assessment of metabolic time-scales within living plant tissues and provides a valuable complement to steady state flux determinations.

Keywords: *Linum usitatissimum*; Oilseed embryo; Carbon-13 labelling experiments; Nuclear magnetic resonance; Metabolic fluxes; Metabolic steady state; Isotopic steady state

1. Introduction

^{13}C-labelling strategies have been increasingly used over the past three decades to investigate carbon metabolism in plants. The method can be applied to identify the metabolic fate of specific substrates to evaluate the effects of environmental factors or genetic backgrounds on carbon metabolism. Steady state ^{13}C-labelling experiments have been introduced more recently for the analysis of metabolic fluxes in plant tissues (Dieuaide-Noubhani et al., 1995, 1997; Rontein et al., 2002; Schwender and Ohlrogge, 2002; Thelen and Ohlrogge, 2002; Schwender et al., 2003; Sriram et al., 2004). The method has been reviewed recently and provides a promising tool for the functional analysis of plant metabolic networks in the framework of systems biology approaches (Roscher et al., 2000; Kruger et al., 2003; Schwender et al., 2004; Ratcliffe and Shachar-Hill, 2006).

In ^{13}C-labelling experiments, fluxes are estimated on the basis of the label distribution in metabolites from plant material incubated with ^{13}C-labelled substrates, using more or less complicated mathematical models (Wiechert, 2001). Current strategies are applicable to metabolic and isotopic

* Corresponding author. Tel.: +33 0 322 827 471; fax: +33 0 322 827 595.
E-mail address: albrecht.roscher@u-picardie.fr (A. Roscher).
[1] Institute of Biomedical and Life Sciences, University of Glasgow, Glasgow G12 8QQ, United Kingdom.

0031-9422/$ - see front matter © 2007 Elsevier Ltd. All rights reserved.
doi:10.1016/j.phytochem.2007.04.018

steady-state conditions, i.e. conditions where both intermediates and fluxes are stable and label enrichment in all intermediates is constant, which provides both analytical and mathematical simplifications (Fernie et al., 2005). Though most flux determinations only use steady state data, there are at least two good reasons to measure the kinetics of label incorporation. First, when steady state labelling experiments are carried out for the purpose of metabolic flux analysis, the isotopic and metabolic steady states have to be ascertained in appropriate ways to avoid misinterpretation of the labelling data. Second, the kinetics of label incorporation contain much greater information regarding the actual rates of biochemical reactions in the metabolic network compared with the steady state conditions, since some unidirectional fluxes that cannot be determined from steady state data are accessible from dynamic labelling data.

The kinetics of ^{13}C-label incorporation can be obtained from *in vitro* NMR or MS analysis of metabolites extracted at different time intervals during time-course labelling experiments carried out *in vivo* (Dieuaide-Noubhani et al., 1995; Schwender et al., 2003). NMR provides an additional alternative, since it allows *in situ* investigations to be conducted on living material. This makes it possible to carry out time-course labelling experiments on a single batch of plant material from which real-time, *in situ* assessment of the kinetics of label incorporation and subsequently a steady state analysis can be performed. In this work, we present the kinetics of ^{13}C-label incorporation in developing linseed embryos, taking advantage of the occurrence of large metabolite pools in this tissue to provide direct and quantitative measurement of their labelling status. The purpose of the work was: (i) to determine the time needed to obtain both metabolic and isotopic steady states in ^{13}C-labelling experiments, (ii) to provide information on metabolic time-scales in living plant tissues, and (iii) to measure metabolic fluxes that cannot be obtained at isotopic steady state. It is exemplified here with oilseed embryos, which are increasingly studied using ^{13}C-labelling strategies to get insight into the efficiency of fatty acid synthesis (Schwender and Ohlrogge, 2002; Schwender et al., 2003, 2006; Sriram et al., 2004).

2. Results

2.1. Metabolic status of incubated embryos

The time-course of lipid accumulation in linseed seeds was measured with pulsed low field NMR of dry seeds (data not shown). The rate of oil accumulation was maximum and almost constant (0.17 mg embryo^{-1} day^{-1}) over a period ranging from 15 to 27 DAF (days after flowering) and embryos were collected at 17–24 DAF to carry out *in vivo* NMR experiments. Collected embryos were dissected, placed on a filter plate in an 8 mm NMR tube and perfused with an oxygenated oilseed embryo incubation medium optimised for *in vivo* NMR investigations (see Section 5 for details). The metabolic status of the embryos was evaluated in two ways. First, the energetic status was assessed from an *in vivo* ^{31}P NMR spectrum at the beginning of each experiment, during which the signals from ATP could always be clearly detected (data not shown). In a long-term ^{31}P NMR experiment, ATP signals remained constant over 48 h of incubation, indicating that the embryos could maintain a stable energy metabolism during such a period of time. No evidence for intracellular acidification, i.e. no shift of the cytosolic inorganic phosphate peak, was observed. This indicates that the incubation conditions – 100% O_2 supply and 7 mL min^{-1} medium flow rate – avoided local hypoxia in the tightly packed embryos. Second, the rate of lipid synthesis was evaluated from the evolution of the intensity of fatty acid signals in time-course ^{13}C NMR experiments (see below) and compared with the rate measured *in planta*. Incubated linseed embryos accumulated lipids at a rate representing 118 ± 18 % ($n = 4$) of the rate measured *in planta*. Taken together, these observations indicate that dissected embryos are viable, metabolically active and stable for at least 48 h in our incubation conditions.

2.2. The natural abundance ^{13}C NMR spectrum

At the start of the experiment, embryos were incubated for 1 h in a medium containing unlabelled glucose to collect natural abundance ^{13}C NMR data. A typical spectrum obtained with linseed embryos is given in Fig. 1. It contains signals from components of the incubation medium, including the osmoticum – sorbitol, MES buffer and unlabelled glucose, and from the most abundant internal compounds, including mainly sucrose and lipids (see insets of Fig. 1). The peaks from storage lipids could be assigned accurately, enabling the major fatty acids to be identified. The composition in fatty acids obtained in such a way was approximately C16:0 + C18:0 = 19%, C18:1 = 12%, C18:2 = 29%, C18:3 = 40% which is consistent with values for linseed oil from mature grains (9%/17%/14%/60%) (Harwood, 1998).

2.3. Real-time monitoring of ^{13}C NMR labelling kinetics in linseed embryos

After 1 h of incubation, the unlabelled glucose in the medium was substituted by [1-^{13}C]glucose, and the incorporation of label into different metabolites was monitored with a time resolution of 0.5 h.

2.3.1. Lipids

After addition of the labelled sugar, a strong increase in the peaks from all even-numbered carbons of fatty acids was observed (Fig. 2). The incorporation of label into these positions is consistent with the expected labelling of the methyl group of acetyl-CoA from [1-^{13}C]glucose. A slight increase was also observed for the signals from odd-num-

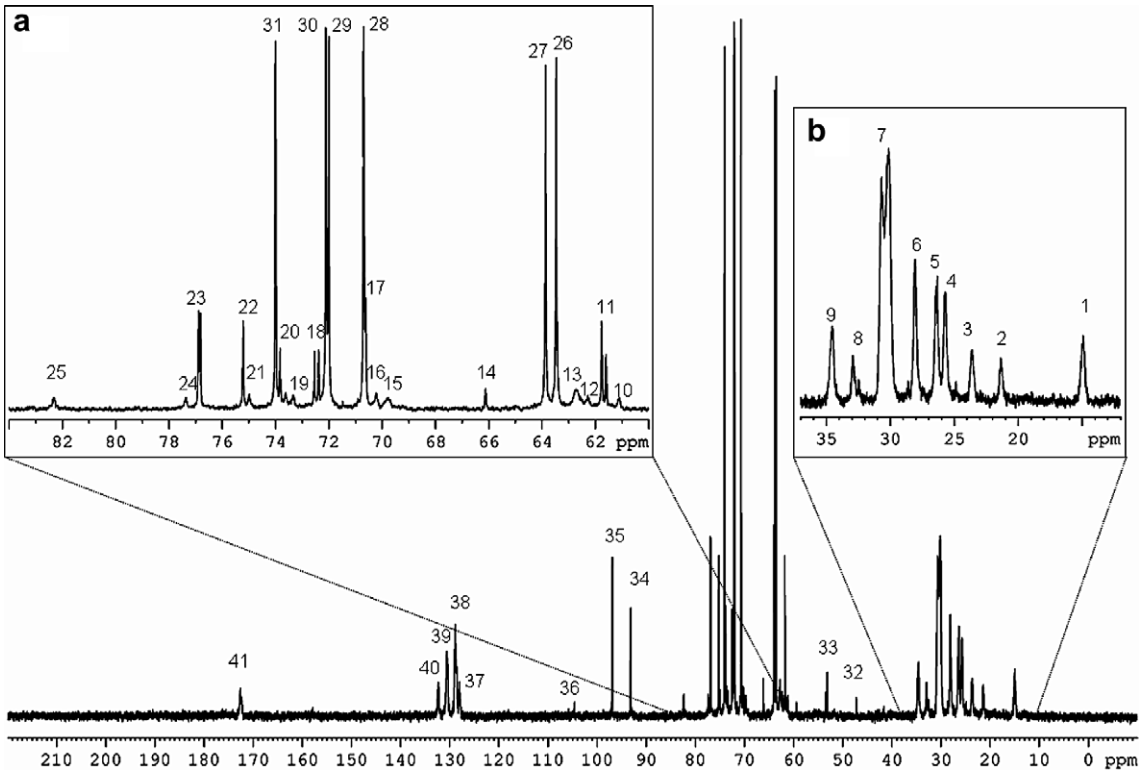

Fig. 1. *In vivo* natural abundance ^{13}C NMR spectrum of developing linseed embryos. Inset a: spectral region (60–84 ppm) displaying most sugar resonances. Peak assignments: Giα, Giβ, Sif and Sig correspond to carbon number i of α and β glucose and of the fructosyl and the glucosyl moieties of sucrose. 10 S6g; 11 G6α; G6β; 12 S1f; 13 C1 and C3 of glycerol from triglycerides; 14 MES; 15 C2 of glycerol from triglycerides ; 16 S4g; 17 G4α and β; 18 G2α and G5α; 19 S3g and S5g; 20 G3α; 21 S4f; 22 G2β; 23 G3β and G5β; 24 S3f; 25 S5f; 26–31 sorbitol. Inset b: spectral region (12–37 ppm) displaying mostly lipid saturated carbon resonances. Peak assignments: 1 Terminal methyl group of all fatty acids (C16 or C18); 2 C17 of linolenic acid (C18:3); 3 C15 of palmitic acid (C16:0) and C17 of stearic acid (C18:0), oleic acid (C18:1) and linoleic acid (C18:2); 4 C3 (all); 5 C11 (C18:2 and C18:3) + C14 (C18:3); 6 C8 (C18:1, C18:2 and C18:3) + C11 (C18:1) + C14 (C18:2); 7 C4 to C7 (all) + C8 to C13 (C16:0) + C8 to C15 (C18:0) + C12 to C15 (C18:1) + C15 (C18:2); 8 C14 (C16:0) and C16 (C18:0, C18:1 and C18:2); 9 C2 (all). Further peaks of interest are: 32 and 33 MES; 34 G1α and S1g; 35 G1β; 36 S2f; 37 C15 (C18:3); 38 C10 and C12 (C18:2 and C18:3) and C13 (C18:3); 39 C9 (C18:1, C18:2 and C18:3), C10 (C18:1) and C13 (C18:2); 40 C16 (C18:3); 41 C1 (all fatty acids).

bered carbons. Storage lipids continuously accumulate as end-products of metabolism in developing linseed embryos. At metabolic steady state, the accumulation is expected to be linear. This can be verified from the time-curve of ^{1}H NMR spectra (data not shown) and was found to be the case except for a slight decrease in the accumulation rate for the last 5–6 h of the experiment. The signals from the terminal methyl carbons (C18 or C16) of fatty acids (Fig. 2, inset) evolved also in a linear manner with a short lag phase after addition of the label, and a slight drop in slope for the last hours. This increase in the even-numbered carbons of fatty acids results from both lipid accumulation and incorporation of label from the metabolic precursor, i.e. the methyl group of plastidic acetyl-CoA, and the linearity shows both metabolic steady state for the rate of lipid synthesis and isotopic steady state for the acetyl-CoA pool. The observed lag phase corresponds to the time necessary for establishment of the isotopic steady state.

When the specific enrichment of the precursor and the amount of lipid per embryo are known, the slope directly reflects the rate of lipid synthesis. The enrichment of the C2 of acetyl-CoA was assumed to be the same as the enrichment in the C3 of alanine, both being derived from the C3 of pyruvate. The latter was evaluated from ^{1}H NMR spectra of the perchloric acid (PCA) extracts to be $35 \pm 3\%$ which is consistent with the mean enrichment of the C1 and C6 from hexose phosphates, the metabolic precursors via glycolysis, as measured from sucrose (Table 1). With this value and the amount of lipids per embryo taken from the accumulation curve, we found a rate of lipid synthesis of 0.20 ± 0.03 mg embryo^{-1} day^{-1} ($n = 4$), i.e. $118 \pm 18\%$ of the *in planta* rate.

2.3.2. Sucrose

Fig. 3 shows the incorporation of label into sucrose. The increase is obvious for the C1 and C6 from both glucosyl (S6g) and fructosyl (S1f, S6f) moieties of sucrose. S1g is also heavily labelled as can be seen from the extract spectra, but this is difficult to follow *in vivo* since the peak overlaps with the C1 peak from α-glucose. Other carbon positions showed little (C3) or no apparent (C2, C4 and C5) incorporation of label. Some peaks like S5f or S2f split partially into a doublet due to *J*-coupling with a neighbouring ^{13}C (S6f and S1f, respectively). This has to be taken into account for peak integration. Labelling at C1 is due to direct conversion of [1-^{13}C]glucose into hexose phos-

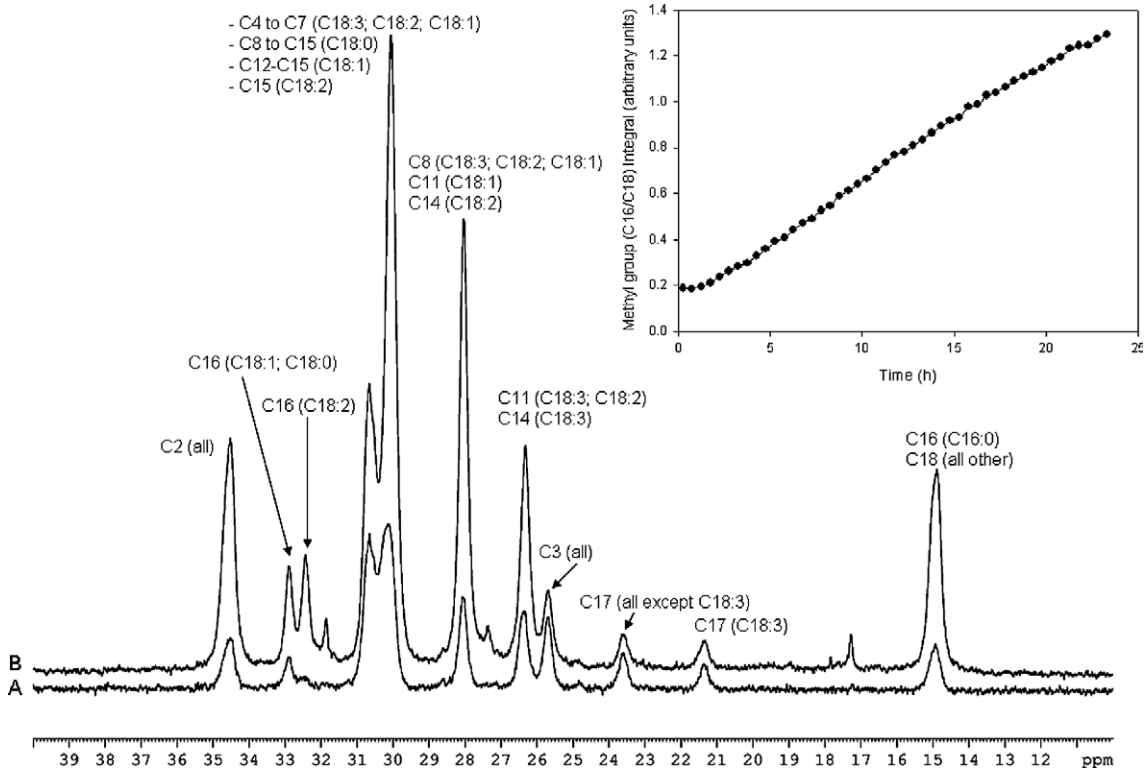

Fig. 2. Spectral region displaying lipid resonances at natural abundance (A) and after 23 h incubation with [1-^{13}C]glucose (B). The insert shows the ^{13}C incorporation in the terminal methyl group of fatty acids (C18 or C16) expressed in arbitrary units during the *in vivo* NMR experiment.

Table 1
Comparison of specific enrichments of sucrose measured *in vivo* and *in vitro* ($n = 4$)

	In vivo	*In vitro*
S1f	53.7 ± 5.3 %	54.0 ± 1.9 %
S6g	13.4 ± 1.1 %	13.1 ± 2.6 %
S6g/S1f	0.25 ± 0.02	0.24 ± 0.04

S1f and S6g denote carbons C1 of the fructosyl and C6 of the glucosyl moiety of sucrose, respectively.

phates and then sucrose. The labelling at C6 is usually observed in plants and comes from the reversibility of reactions in the upper part of glycolysis (Hatzfeld and Stitt, 1990; Fernie et al., 2001) and of transaldolase (Dieuaide-Noubhani et al., 1995). The slight labelling at C3 comes from cycling around the reversible reactions of the non-oxidative branch of the pentose phosphate pathway (Roscher et al., 2000). The C2, C4 and C5 positions have a low probability to be labelled from [1-^{13}C]glucose (Roscher et al., 2000). Indeed, labelling of C2 can only derive from C3-labelled hexose phosphate submitted to a further full cycle through either the oxidative or the non-oxidative branch of the pentose phosphate pathway. Label in C4 and C5 like the label in C6 comes only from re-synthesis of hexose phosphates from triose phosphates, and the C4/C3 and C5/C2 ratios should therefore be the same as the C6/C1 ratio, i.e. 25% (Table 1). Furthermore, peaks due to labelled fructose appear in the spectrum (Fig. 3), showing a turnover of sucrose by invertase or sucrose synthase (SuSy). The kinetics of label incorporation in sucrose were obtained by integrating relevant peak areas over all the incubation period. The results are illustrated in the inset of Fig. 3 for the most interesting signals (S1f, S6g and S5f). After an initial decrease, the S5f signal increased during the first 18 h of the experiment to become stable by the end of the experiment. Because the C5 position was not or was at most very feebly labelled, its evolution reflects an increase in the sucrose pool to reach a steady state concentration 18 h after the start of the incubation. The peak intensity increased in two phases for both S1g and S6f signals to reach a plateau at 18 h of labelling. This bi-phasic behaviour might be explained by a first rapid labelling of the cytosolic sucrose pool and a slower labelling of the larger vacuolar sucrose pool. Interestingly, the ^{13}C incorporation into fructose starts with a lag phase of 2 h and then increases linearly for 18 h and finally reaches a plateau (data not shown) confirming continuous turnover of the sucrose pool. Together, these results indicate that both metabolic and isotopic steady states were reached at the level of sucrose 18 h after the addition of the labelled substrate, under our experimental conditions. Interestingly, the peak ratio between S6g and S1f (Fig. 4a) reached a steady state value only 3 h after addition of the [1-^{13}C]glucose. This confirms that the hexose phosphate pool is already at isotopic steady state at this early point. The steady state values obtained (Table 1) are compatible with measurements on the corresponding PCA extracts.

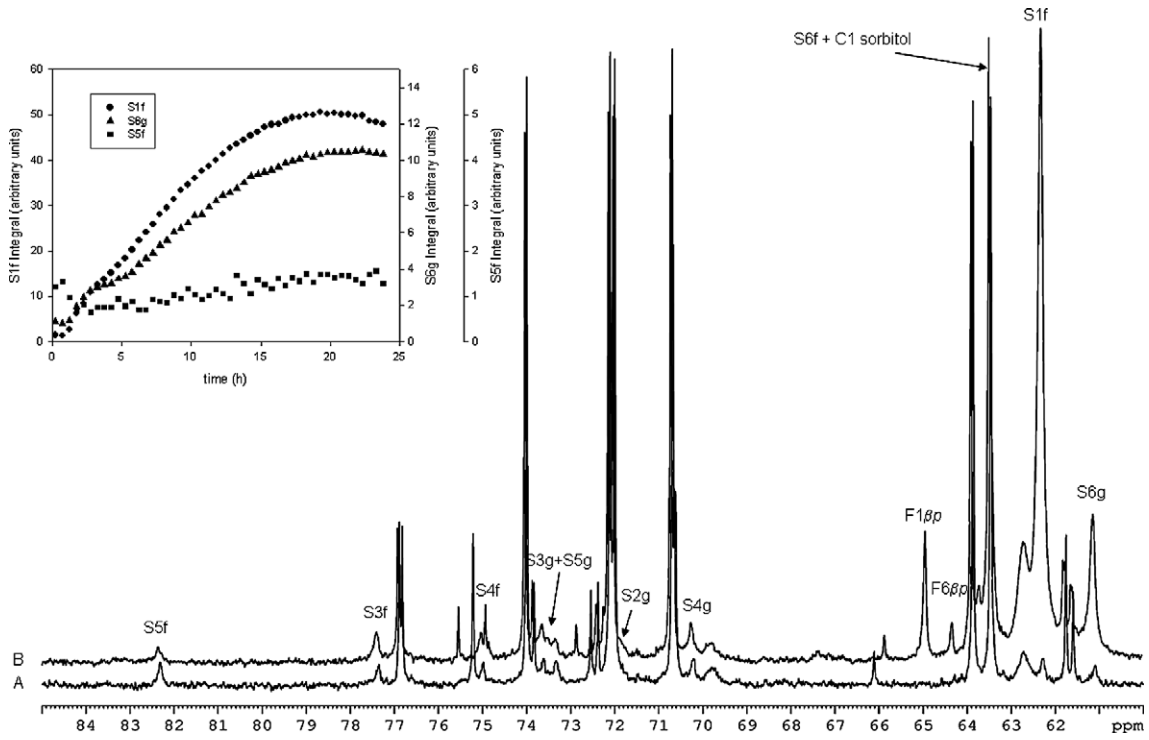

Fig. 3. Spectral region displaying sucrose resonances at natural abundance (A) and after 23 h incubation with [1-^{13}C]glucose (B). Sif and Sig, resonances of carbon number i of the glucosyl and fructosyl moieties of sucrose. Fiβp, resonance of carbon number i of the β-pyranose form of fructose. The insert shows the ^{13}C incorporation in S1f (circles), S6g (triangles) and S5f (squares) expressed in arbitrary units (the same for all three) during the *in vivo* NMR experiment. Note the different scales for the three carbons.

The specific enrichment, i.e. the percentage of ^{13}C label in a given carbon position of the metabolite can also be directly evaluated if an unlabelled peak from the same molecule can be measured at the same time to give a reference. For sucrose in [1-^{13}C]glucose labelling experiments, the best reference peak is that of S5f, since C5 has the lowest probability to become labelled and the fructosyl peak, contrary to the glucosyl peak, is in a spectral region without peak overlap. The referencing is possible if differential relaxation or nuclear Overhauser effects can be avoided or compensated. For *in vivo* experiments, they can hardly be fully avoided because of the short repetition times and continuous ^{1}H decoupling needed to get sufficient signal-to-noise ratios. But, as they remain constant throughout the experiment, they can be compensated for when natural abundance signals can be detected for the compound of interest. Such signals can act as intramolecular reference for natural abundance to measure the enrichment in other positions. Then, the fractional enrichment of a carbon X of sucrose (Sx) can be calculated from the following equation:

$$\mathrm{Sx} = 1.1\% \times (I_{\mathrm{Sx}}/I_{\mathrm{S5f}})_t/(I_{\mathrm{Sx}}/I_{\mathrm{S5f}})_{\mathrm{un}}$$

where $(I_{\mathrm{Sx}}/I_{\mathrm{S5f}})_t$ is the intensity ratio for carbons X and S5f, respectively, at a time t of the experiment and $(I_{\mathrm{Sx}}/I_{\mathrm{S5f}})_{\mathrm{un}}$ the same ratio in the reference spectra obtained when the embryos were fed with unlabelled glucose.

Using this method, the evolution of the specific enrichments during the course of the labelling experiment could be monitored, as shown in Fig. 4b for S1f and S6g. For both carbons, the enrichment increased for 9 h after addition of the labelled substrate. The increase was bi-phasic, 2 h of rapid increase and then about 7 h of slower increase, possibly corresponding to a rapid renewal of cytosolic sucrose and a slower turnover of vacuolar sucrose. Then, the ^{13}C enrichment remained stable for at least 13 h. The specific enrichments measured at the plateau for S1f and S6g were $53.7 \pm 5.3\%$ and $13.4 \pm 1.1\%$ ($n = 4$), respectively (Table 1). These values were compared with the specific enrichments determined from sucrose extracted from the embryos at the end of the labelling experiment (*in vitro* measurements). For both S1f and S6g, the enrichments measured *in vivo* were similar to those measured *in vitro*, albeit with lower precision (Table 1). Such results demonstrate the accuracy of the proposed method to provide *in vivo* measurements of specific enrichments, though it should be stressed that this measurement relies on the strict assumption that the reference peak remains unlabelled and does not overlap with any peak, even a small one. Therefore, absolute values might be compromised in specific cases but the time-course to follow progress to isotopic steady state is still valid.

Taken together, the above results indicate that isotopic steady state was achieved within the sucrose pool 9 h after the addition of the label. Complete metabolic and isotopic steady state was reached after 18 h, as schematised in Fig. 5.

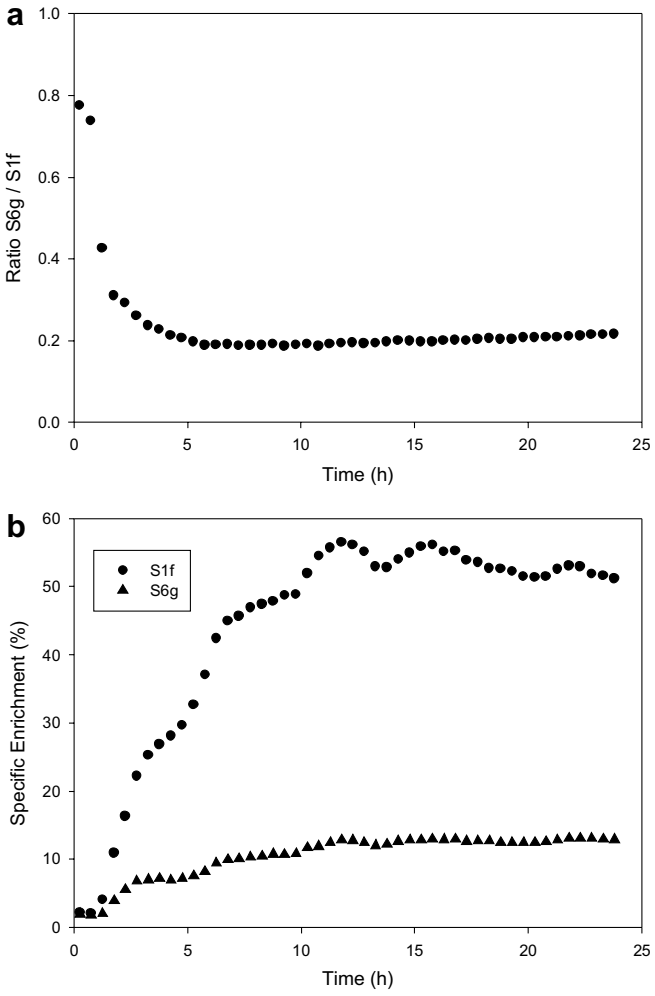

Fig. 4. (a) Evolution of the S6g/S1f ratio during ^{13}C-labelling experiment carried out *in vivo*. This ratio is representative of the equilibration of label within the upper part of glycolysis (between hexose phosphates and triose phosphates). The ratio evolved within the first 3 h of the labelling experiment and became stable afterwards, indicating the equilibration of label to be complete at this level. (b) Evolution of the ^{13}C enrichment of S1f and S6g. Enrichment is given as the percentage of label within carbons C1 of the fructosyl moiety (S1f, circles) and C6 of the glucosyl moiety (S6g, triangles) of sucrose.

The sucrose label kinetics can also be used to derive metabolic flux information that is not available from steady state experiments. Indeed, the same type of steady state experiment can only determine the rate of sucrose cycling via invertase (Dieuaide-Noubhani et al., 1995; Rontein et al., 2002), and this only if flux through glucose 6-phosphatase can be excluded (Alonso et al., 2005), whereas the dynamic labelling information from the *in vivo* experiment gives information on the rate of sucrose synthesis and can even discriminate between action of sucrose 6-phosphate synthase (SPS) and SuSy. Indeed SuSy uses fructose and UDPglucose as substrates, and can therefore only result in labelling of the glucosyl moiety of sucrose, whereas SPS uses Fru6P and thus labels also the fructosyl moiety. The flux through SPS can therefore be deduced from the initial slope of the ^{13}C-incorporation curve for

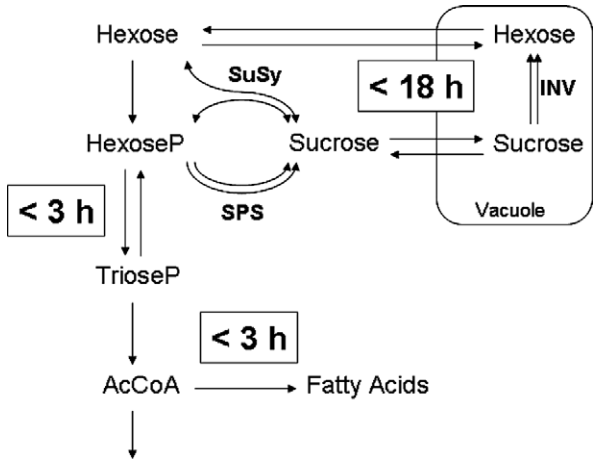

Fig. 5. Metabolic time-scales in linseed embryos. Schematic representation of the time needed to obtain label equilibration within linseed embryo metabolism during ^{13}C-labelling experiments. The equilibration of label within central pathways (glycolysis to acetyl-CoA) was complete within 3 h, while complete metabolic and isotopic steady states for sucrose needed 18 h.

S1f and the enrichment of the precursor, i.e. C1 of Fru6P. The latter is determined precisely from the steady state enrichment of S1f in the PCA extract. The resulting rate is estimated to be 3.1 ± 1.0 μmol embryo^{-1} h^{-1}. The same approach with S6g yields the combined SPS and SuSy rate at 3.0 ± 1.2 μmol embryo^{-1} h^{-1} meaning that the sucrose synthesis flux is dominated by SPS. This synthesis rate is in good agreement with sucrose fluxes found in other plant tissues (Sweetlove et al., 2002; Alonso et al., 2005) from dynamic ^{14}C-labelling but more importantly we show that the use of both *in vivo* and *in vitro* NMR gives a direct and reliable way of measuring the rate of sucrose synthesis in the incubated plant material.

3. Discussion

In vivo NMR provides an almost unique opportunity to investigate metabolism in a non-invasive manner. As shown in this study, this makes *in vivo* NMR a suitable method to monitor *in situ* the kinetics of label incorporation during ^{13}C-labelling experiments. In principle, the approach can be applied to various biological systems, but it is particularly well adapted to plant material. The application of *in vivo* NMR to plant tissues is favoured by the rather long metabolic time-scales (over hours) encountered in plants, enabling time-course experiments to be carried out with accurate time resolution and signal-to-noise ratios. Plant systems also accumulate NMR detectable reserve material (e.g. sucrose, lipids, free amino acids and organic acids) to a large extent, which provides valuable compounds to examine the evolution of the labelling state of intermediate metabolites. In many cases, the size of the reserve pools is sufficient for carbons at natural abundance to be detected properly, from which the ^{13}C enrichment of labelled positions in the same metabolite

can be determined. The potential accuracy of such an 'intramolecular referencing' approach to provide quantitative analysis of label incorporation is shown in this work by the close agreement of sucrose enrichments determined *in vivo* with the ones measured after extraction of the sugar but, in practice, the absolute enrichments are also available with greater confidence from extracted material. The relative time-course of enrichments, however, provides information that otherwise is not readily accessible.

Where it can be applied, the above strategy provides several unique features in the context of ^{13}C-labelling experiments, including the possibility to assess *in situ* the establishment of metabolic and isotopic steady states on a single batch of material. For the purpose of metabolic flux analysis, one can monitor the labelling status of the plant material during the *in situ* NMR investigation through the specific enrichments of reserve compounds and make the decision to stop the experiment once the enrichments have remained constant for a couple of hours. Then, metabolites useful for flux analysis can be extracted and their labelling pattern measured in detail by relevant techniques (NMR and/or MS). This avoids the need for a series of labelling experiments to be carried out on independent batches to establish the time course evolution of the label, thereby saving time, label, and effort. Problems linked to biological variability are also reduced because a batch of material is its own control for the establishment of steady state.

The method presents a number of limits as well, including the general limits to the use of NMR for metabolic investigations in living systems (availability of a NMR spectrometer, capability to maintain the biological material in a reasonably stable physiological state, difficulty of illumination, amount of material needed for accurate signal-to-noise ratios, etc.) (Ratcliffe et al., 2001). The analysis is restricted to the most abundant metabolites, preferably to those for which natural abundance signals are detectable. For a given biological system, the purpose of the investigation must be consistent with the nature of the metabolites that are actually detected, and a steady state cannot be assumed for parts of the metabolic network that are not accessible. Thus, the number and nature of the compounds for which quantitative isotopic information can be obtained during the course of the *in vivo* experiments determines the nature and size of the metabolic network that can actually be investigated.

In linseed embryos, the availability of both sucrose and lipid signals enabled the labelling kinetics to be monitored in both the upper (sucrose) and lower (lipids) parts of central metabolism. From the data obtained, the kinetics of label incorporation could be examined at different levels of metabolism (see Fig. 5). The evolution of the lipid signals indicated the pool of acetyl-CoA used for fatty acid synthesis to be in a stable isotopic state 3 h after the addition of label. Such a fast equilibration of label could be also evidenced in the upper part of glycolysis. More specifically, the stability of the S6g/S1f labelling ratio indicated that hexose phosphates and triose phosphates fully equilibrated within a similar period of time. This time is probably dominated by equilibration of label in the intracellular glucose pool since the phosphorylated glycolytic intermediates have turnover times in the order of seconds (Roscher et al., 1998). The equilibration of label between hexose phosphates and sucrose took a much longer time: the specific enrichment of sucrose carbons became stable only 9 h after the addition of label. The evolution of the sucrose signals was also useful to determine the rate of sucrose synthesis and showed that the sizeable sucrose pool needs 18 h to stabilise. In other words, it could be reasonably concluded that after 18 h the rate of sucrose use has exactly balanced the rate of sucrose synthesis and that metabolic steady state has been reached. This result is consistent with previously studies on plant tissues showing that steady state labelling in metabolites takes some hours to be established when labelled substrates are supplied (Salon et al., 1988; Dieuaide-Noubhani et al., 1995; Edwards et al., 1998; Alonso et al., 2005). These data also show that the label equilibration within the central metabolic network is much faster than complete equilibration of the reserve pools and that sucrose itself, as a large reservoir, is a good reporter for steady state in embryo metabolism and, presumably, other plant systems. It should be noted that sucrose turnover will dilute the hexose and hexose phosphate pools until sucrose itself is at isotopic steady state, so that these pools are only at steady state when sucrose is. However this effect is apparently too small to be readily seen with *in vivo* NMR.

This highlights a problem in the recent tendency in steady state flux analysis in plants to analyse the labelling in large reserve pools (proteins, lipids, etc.) accumulated over several days, a period for which metabolic steady state is uncertain as developmental shifts in reserve accumulation occur (Eastmond and Rawsthorne, 2000). This situation is different from flux analysis in micro-organisms that can be cultured for several generations.

Before metabolic steady state is reached, real-time incorporation curves go through a transient status, which can be valuable to determine fluxes inaccessible under steady state conditions. The labelling of both moieties of sucrose shows that at least some part of sucrose is synthesised through the sucrose phosphate synthase (SPS) reaction from the cytosolic hexose phosphate pool. However, at isotopic steady state, the fructosyl moiety of sucrose, free fructose and fructose 6-phosphate show similar enrichments, and this means that the rate of sucrose synthesis cannot be directly measured once the steady state is reached. Using isotopic labelling, two methods have so far been developed to quantify this flux. Historically, short-time feeding experiments using radioactive substrates were used to determine the unidirectional flux of sucrose synthesis from the rate of incorporation of radioactivity into sucrose (Hatzfeld and Stitt, 1990; Hargreaves and ap Rees, 1988, 1994, 1995; Sweetlove et al., 2002). This method has been used recently (Alonso et al., 2005), and as mentioned by these authors, this approach relies on the ability to determine accurately the specific radioactivity of the precursor (hexose phos-

phate pool) and to ensure that no radioactivity is lost by degradation reactions – i.e. SuSy and invertase reactions. A second approach was developed using steady state labelling experiments where a lower boundary can be put on the rate of sucrose synthesis by measuring sucrose hydrolysis through invertase (Dieuaide-Noubhani et al., 1995; Rontein et al., 2002). In the present work, a third approach is validated. Using the kinetics of ^{13}C-label incorporation into sucrose before the steady state is reached, we show that it is possible to measure directly the flux through the synthesis reactions – i.e. SPS and SuSy.

4. Conclusion

This study shows that *in vivo* NMR can be employed to investigate the *in situ* kinetics of ^{13}C-label incorporation in plant systems in a quantitative manner. In developing linseed embryos, the equilibration of label within the intermediate pathways took less than 3 h whereas complete metabolic steady state took 5–6 times longer to be reached. The transient period between label equilibration and metabolic equilibration can be profitably used to determine fluxes that cannot be determined during the complete steady state. This makes the approach suitable to gain a better understanding of metabolic regulation and a comprehensive assessment of the metabolic pathways that occur in cells and tissues.

5. Experimental

5.1. Plant material

Plants of linseed (*Linum usitatissimum* L., cv. Barbara) were grown in a greenhouse at 18 °C under a 16 h photoperiod in daylight supplemented by sodium light. The age of linseed embryos was determined by tagging each new flower every day and expressed as days after flowering (DAF).

5.2. Lipid accumulation

Linseed capsules aged 15–42 DAF were harvested. Collected seeds were weighed (≈200 mg) and oven-dried at 100 °C overnight. Lipid content was determined using pulsed low-field NMR (Oxford QP20+/PC, 20 MHz) on the basis of dry weight in general accordance with the guideline ISO 10565 (International Standardisation Organisation, 1993). Quantification was carried out directly on the FIDs by comparison with canola seed standards supplied by the Canadian Grain Council (Hobbs et al., 2004; Chia et al., 2005).

5.3. In vivo NMR experiments

Capsules containing seeds at the appropriate stage of development were harvested and dissected. During dissection (up to 2 h), embryos without testa were kept on ice in a modified Nitsch and Nitsch culture medium (Hill et al., 2003) composed of $Ca(NO_3)_2$ 500 mg L^{-1}, KNO_3 125 mg L^{-1}, KH_2PO_4 125 mg L^{-1}, $MgSO_4$ 125 mg L^{-1}, H_3BO_3 10 mg L^{-1}, $ZnSO_4$ 10 mg L^{-1}, Na_2MoO_4 250 μg L^{-1}, $CoCl_2$ 25 μg L^{-1}, $CuSO_4$ 25 μg L^{-1}, L-glutamine 800 mg L^{-1}, L-serine 100 mg L^{-1} and nicotinic acid 5 mg L^{-1}. Fe and Mn ions (paramagnetic properties in NMR) and minor organic elements only necessary for long-term growth were left out from the initial composition of the culture medium. The medium was buffered at pH 6 with MES 10 mM. Finally, 250 mM sucrose was added as a carbon source and as an osmoticum (The osmotic pressure of the incubation medium is an important factor influencing embryo development without testa. The maintenance of a high osmotic pressure is a prerequisite for complete embryonic development without precocious germination (Johnson et al., 1997)). At the end of the dissection, embryos were rinsed three times with the modified medium containing 250 mM of sorbitol, a non-metabolisable sugar, instead of sucrose ("sorbitol medium").

During *in vivo* NMR experiments, the dissected embryos were perfused in the NMR tube with oxygenated nutrient medium at room temperature. The perfusion system consisted of a septum screw cap 8 mm NMR tube, an outside reservoir and a peristaltic pump connected by flexible tubing (Tygon). The embryos (∼150) were tightly packed on a filter plate made from expanded polyethylene (Vyon) in the detection region of the NMR tube. The re-circulating medium was pumped with a peristaltic pump at 7 mL min^{-1} to the top of the NMR tube arriving through a syringe needle placed through the septum. After passage through the sample, the medium left the NMR tube through a central glass capillary connecting the bottom of the tube to a syringe needle through the septum. The medium was bubbled in the reservoir by pre-humidified O_2. At the beginning of the *in vivo* experiment, 30 mL of medium containing 250 mM sorbitol and 100 mM unlabelled glucose were circulated through the sample. The total sugar concentration (350 mM of glucose + sorbitol) was similar to the concentration reported for rapeseed endosperm (Hill et al., 2003). After having acquired ^{31}P, ^{13}C and ^{1}H reference spectra, the embryos were rinsed with fresh sorbitol medium to remove the unlabelled glucose and then 100 mM [1-^{13}C]glucose was added as a carbon source (labelled glucose medium). NMR spectra (see below) were then collected in successive blocks for 24–48 h. After 48 h, approximately 70% of the initial glucose concentration was still detected in the incubation medium indicating a constant nutrient supply over the time-course of the experiment.

NMR spectra were obtained on a Bruker Avance 300 wide bore spectrometer with an 8 mm broadband probehead. At the start of each experiment, one ^{31}P spectrum was recorded (121.49 MHz, 45° pulse angle, interpulse delay 0.5 s, power gated WALTZ 16 ^{1}H decoupling) to assess the energetic state of the embryos. During the rest

of the experiment, one ^{1}H spectrum (300.13 MHz, 4 min) with water presaturation and two ^{13}C spectra (75.47 MHz, 28 min) were acquired per hour. ^{13}C spectra were recorded as follows: 60° pulse angle (5.5 μs), interpulse delay 1.5 s, power-gated WALTZ 16 ^{1}H decoupling. The FIDs were zero-filled and exponentially multiplied (1 or 4 Hz) before Fourier transformation and integration. Peaks were assigned according to spectroscopic tables (Fan, 1996) and comparison with standard compounds.

5.4. PCA extraction and in vitro NMR experiments

At the end of the *in vivo* experiment, the embryos were collected, rinsed, weighed and frozen in liquid nitrogen. Extraction of the soluble metabolites followed a protocol adapted from Aubert et al. (1997). The frozen plant material was quickly ground to a fine powder in a mortar with 0.5 mL (g FW)$^{-1}$ of 3 M perchloric acid (PCA). As an extraction standard for quantification, 50 μL of formic acid 1 M were added. Divalent cations (particularly Mg^{2+} and Mn^{2+}) were chelated by the addition of 20 μL (g FW)$^{-1}$ of 0.5 M EDTA. The frozen powder was transferred into a centrifuge tube and thawed slowly on ice. To obtain a homogeneous suspension, a sufficient amount of ice-cold 1 M PCA was then added (typically 5 mL for 1 or 2 g of sample). The thick suspension was centrifuged 20 min at 20,000 rpm and the supernatant retained. Then, the same amount of 1 M PCA was added to the pellet, homogenised and centrifuged as above. The final extraction was performed with H_2O instead of PCA and centrifuged under the same conditions. The pellet was dried under nitrogen flux and kept at −80 °C. The combined supernatants were neutralised with 2 M $KHCO_3$ to about pH 5 and centrifuged as above. The resulting supernatant was freeze-dried, dissolved in 2.5 mL of water and centrifuged 2 min at 14,000 rpm. Before being used for measurements, the supernatant was buffered with phosphate buffer (final concentration 50 mM) pH 7.5 and centrifuged as above. For NMR measurements, the supernatant was collected, freeze-dried and resuspended in 500 μL of D_2O.

^{13}C NMR spectra were obtained at 75.47 MHz with a 5 mm DUAL $^{13}C/^{1}H$ probe. ^{13}C acquisition parameters were: 90° pulse angle (5.5 μs), interpulse delay 61 s with ^{1}H decoupling. ^{1}H NMR spectra were obtained at 300.13 MHz with the same probe using a 90° pulse angle (6.5 μs) and an interpulse delay of 5 s.

5.5. Sucrose ^{13}C specific enrichment calculation

The absolute enrichment of S1g was determined from the ^{1}H spectra as the ratio of the area of the ^{13}C-satellites to the total area of the multiplet. The relative enrichment of the other sucrose carbons was determined from ^{13}C spectra and calibrated from the absolute enrichment of S1g determined by ^{1}H NMR. Peak areas were determined by integration.

5.6. Rate of sucrose synthesis

^{13}C-incorporation curves have been obtained by integrating each sucrose peak during the entire experiment. Using the formic acid added to the frozen embryos as an internal standard before extraction, the real-time kinetics originally obtained in arbitrary units have been expressed in μmol embryo^{-1}. The rates of ^{13}C-incorporation into S1f and S6g were determined from the slope of the curve between 0 and 5 h after addition of the labelled glucose. The S1f integrals were corrected for the contribution from the neighbouring glycerol C1/C3 peak. The rates were converted to sucrose synthesis rates by dividing with the precursor ^{13}C-enrichment determined on the extract (Table 1).

Acknowledgements

We thank Dr Douglas Hobbs and Dr Tansy Chia for help in the lipid accumulation analysis and Dr Dominique Cailleu for maintenance of the 300 MHz NMR spectrometer. The EU contributed financially to this research project (QLK3-2000-00349). S.T. gratefully acknowledges financial support for her Ph.D. from Alternatech, Amiens France. A.R. was recipient of a Marie Curie fellowship (HPMFCT-2000-00672).

References

Alonso, A.P., Vigeolas, H., Raymond, P., Rolin, D., Dieuaide-Noubhani, M., 2005. A new substrate cycle in plants. Evidence for a high glucose-phosphate-to-glucose turnover from *in vivo* steady-state and pulse-labelling experiments with [^{13}C]glucose and [^{14}C]glucose. Plant Physiol. 138, 2220–2232.

Aubert, S., Bligny, R., Day, D.A., Whelan, J., Douce, R., 1997. Induction of alternative oxidase synthesis by herbicides inhibiting branched-chain amino acid synthesis. Plant J. 11, 649–657.

Chia, T.Y.P., Pike, M.J., Rawsthorne, S., 2005. Storage oil breakdown during embryo development of *Brassica napus* (L.). J. Exp. Bot. 56, 1285–1296.

Dieuaide-Noubhani, M., Raffard, G., Canioni, P., Pradet, A., Raymond, P., 1995. Quantification of compartmented metabolic fluxes in maize root tips using isotope distribution from ^{13}C- or ^{14}C-labelled glucose. J. Biol. Chem. 270, 13147–13159.

Dieuaide-Noubhani, M., Canioni, P., Raymond, P., 1997. Sugar-starvation-induced changes of carbon metabolism in excised maize root tips. Plant Physiol. 115, 1505–1513.

Eastmond, P.J., Rawsthorne, S., 2000. Coordinate changes in carbon partitioning and plastidial metabolism during the development of oilseed rape embryos. Plant Physiol. 122, 767–774.

Edwards, S., Nguyen, B.T., Do, B., Roberts, J.K.M., 1998. Contribution of malic enzyme, pyruvate kinase, phosphoenolpyruvate carboxylase, and the Krebs cycle to respiration and biosynthesis and to intracellular pH regulation during hypoxia in maize root tips observed by nuclear magnetic resonance imaging and gas chromatography-mass spectrometry. Plant Physiol. 116, 1073–1081.

Fan, T.W.M., 1996. Recent advances in profiling plant metabolites by multi-nuclear and multi-dimensional NMR. In: Shachar-Hill, Y., Pfeffer, P.E. (Eds.), Nuclear Magnetic Resonance in Plant Biology. American Society of Plant Physiologists, Rockville, MD, pp. 181–254.

Fernie, A.R., Roscher, A., Ratcliffe, R.G., Kruger, N.J., 2001. Fructose 2,6-bisphosphate activates pyrophosphate: fructose-6-phosphate 1-phosphotransferase and increases triose phosphate to hexose phosphate cycling in heterotrophic cells. Planta 212, 250–263.

Fernie, A.R., Geigenberger, P., Stitt, M., 2005. Flux an important, but neglected, component of functional genomics. Curr. Opin. Plant Biol. 8, 174–182.

Hargreaves, J.A., ap Rees, T., 1988. Turnover of starch and sucrose in roots of *Pisum sativum*. Phytochemistry 27, 1627–1629.

Harwood, J.L., 1998. What's so special about plant lipids. In: Harwood, J.L. (Ed.), Plant Lipid Biosynthesis: Fundamentals and Agricultural Applications. Cambridge University Press, Cambridge.

Hatzfeld, W.D., Stitt, M., 1990. Study of the rate of recycling of triose phosphates in heterotrophic *Chenopodium rubrum* cells, potato tubers, and maize endosperm. Planta 180, 198–204.

Hill, S.A., ap Rees, T., 1994. Fluxes of carbohydrate metabolism in ripening bananas. Planta 192, 52–60.

Hill, S.A., ap Rees, T., 1995. The effect of hypoxia on the control of carbohydrate metabolism in ripening bananas. Planta 197, 313–323.

Hill, L.M., Morley-Smith, E.R., Rawsthorne, S., 2003. Metabolism of sugars in the endosperm of developing seeds of oilseed rape. Plant Physiol. 131, 228–236.

Hobbs, D.H., Flintham, J.E., Hills, M.J., 2004. Genetic control of storage oil synthesis in seeds of *Arabidopsis*. Plant Physiol. 136, 3341–3349.

Johnson, R.W., Asokanthan, P.S., Griffith, M., 1997. Water and sucrose regulate canola embryo development. Physiol. Plant 101, 361–366.

Kruger, N.J., Ratcliffe, R.G., Roscher, A., 2003. Quantitative approaches for analysing fluxes through plant metabolic networks using NMR and stable isotope labelling. Phytochem. Rev. 2, 17–30.

Ratcliffe, R.G., Roscher, A., Shachar-Hill, Y., 2001. Plant NMR spectroscopy. Progr. Nucl. Magn. Reson. Spectrosc. 39, 267–300.

Ratcliffe, R.G., Shachar-Hill, Y., 2006. Measuring multiple fluxes through plant metabolic networks. Plant J. 45, 490–511.

Rontein, D., Dieuaide-Noubhani, M., Dufourc, E.J., Raymond, P., Rolin, D., 2002. The metabolic architecture of plant cells. Stability of central metabolism and flexibility of anabolic pathways during the growth cycle of tomato cells. J. Biol. Chem. 277, 43948–43960.

Roscher, A., Emsley, L., Raymond, P., Roby, C., 1998. Unidirectional steady state rates of central metabolism enzymes measured simultaneously in a living plant tissue. J. Biol. Chem. 273, 25053–25061.

Roscher, A., Kruger, N.J., Ratcliffe, R.G., 2000. Strategies for metabolic flux analysis in plants using isotope labelling. J. Biotechnol. 77, 81–102.

Salon, C., Raymond, P., Pradet, A., 1988. Quantification of carbon fluxes through the tricarboxylic acid cycle in early germinating lettuce embryos. J. Biol. Chem. 263, 12278–12287.

Schwender, J., Ohlrogge, J.B., 2002. Probing *in vivo* metabolism by stable isotope labelling of storage lipids and proteins in developing *Brassica napus* embryos. Plant Physiol. 130, 347–361.

Schwender, J., Ohlrogge, J.B., Shachar-Hill, Y., 2003. A flux model of glycolysis and the oxidative pentosephosphate pathway in developing *Brassica napus* embryos. J. Biol. Chem. 278, 29442–29453.

Schwender, J., Ohlrogge, J., Shachar-Hill, Y., 2004. Understanding flux in plant metabolic networks. Curr. Opin. Plant Biol. 7, 309–317.

Schwender, J., Shachar-Hill, Y., Ohlrogge, J.B., 2006. metabolism in developing embryos of *Brassica napus*. J. Biol. Chem. 281, 34040–34047.

Sriram, G., Fulton, D.B., Iyer, V.V., Peterson, J.M., Zhou, R., Westgate, M.E., Spalding, M.H., Shanks, J.V., 2004. Quantification of compartmented metabolic fluxes in developing soybean embryos by employing biosynthetically directed fractional ^{13}C labeling, two-dimensional [^{13}C, ^{1}H] nuclear magnetic resonance, and comprehensive isotopomer balancing. Plant Physiol. 136, 3043–3057.

Sweetlove, L.J., Tomlinson, K.L., Hill, S.A., 2002. The effect of exogenous sugars on the control of flux by adenosine 5′-diphosphoglucose pyrophosphorylase in potato tuber discs. Planta 214, 741–750.

Thelen, J.J., Ohlrogge, J.B., 2002. Metabolic engineering of fatty acid biosynthesis in plants. Metab. Eng. 4, 12–21.

Wiechert, W., 2001. ^{13}C metabolic flux analysis. Metab. Eng. 3, 195–206.